2024 IEEE/ASME International Conference on Advanced Intelligent Mechatronics (AIM)
July 15-19, 2024. Boston, MA, USA

Reachability Analysis of Human-in-the-Loop Systems Using Gaussian Mixture Model with Side Information

Cheng-Han Yang[1], Joonwon Choi[1], Suriyan Anandavel[1], and Inseok Hwang[1]

***Abstract*— In the context of a Human-in-the-Loop (HITL) system, the accuracy of reachability analysis plays a significant role in ensuring the safety and reliability of HITL systems. In addition, one can avoid unnecessary conservativeness by explicitly considering human control behavior compared to those methods that rely on the system dynamics alone. One possible approach is to use a Gaussian Mixture Model (GMM) to encode human control behavior using the Expectation-Maximization (EM) algorithm. However, relatively few works consider the admissible control input ranges due to physical or mechanical limitations when modeling human control behavior. This could make the following reachability analysis overestimate the system's capability, thereby affecting the performance of the HITL system. To address this issue, we present a constrained stochastic reachability analysis algorithm that can explicitly account for the admissible control input ranges. By confining the ellipsoidal confidence region of each Gaussian component using Sequential Quadratic Programming (SQP), we probabilistically constrain the GMM as well as the corresponding stochastic reachable sets. A comprehensive mathematical analysis of how the constrained GMM can affect the stochastic reachable sets is provided in this paper. Finally, the proposed stochastic reachability analysis algorithm is validated via an illustrative numerical example.**

I. Introduction

Reachability analysis has been widely used in the field of cyber-physical systems, as it can ensure the safety of systems. Especially in a Human-in-the-Loop (HITL) system, reachability analysis can significantly enhance the safety of the involved human, such as collision avoidance [1] and loss-of-control prevention of aircraft [2]. However, the existing reachability analysis methods that only rely on the given HITL dynamics might yield overly conservative results. To tackle this problem, one can model the human operator's control behavior using the human control behavioral data. Such a model allows us to predict the human control input at given time steps, and we can incorporate it to improve the accuracy of reachability analysis. For instance, the authors in [1] proposed a method incorporating the human control behavior model. Such incorporation has shown less conservative results, thereby improving the overall system performance and reliability.

One of the major challenges in processing human control behavioral data is the inherent stochastic nature of human actions [3]. In this paper, we select the Gaussian Mixture Model (GMM) as a basis model to address such stochasticity. The GMM has shown better performance with respect to the stochastic features of human control behavior compared to other deterministic approaches [4]. Additionally, the GMM can conform to any trajectories and be used as a generative model [5]. It has also been shown to be an excellent approach to modeling non-Gaussian data [6]. More applications of the GMM for human motion and control behavior modeling can be found in [7]–[9]. With a GMM, one can predict the human control input at a given time step using the Gaussian Mixture Regression (GMR) and further derive the stochastic reachable sets using the Chapman–Kolmogorov equation [1].

Nevertheless, an inappropriately processed human control behavior model could degrade the performance of the reachability analysis [10]. Hence, modeling human control behavior plays a vital role in the HITL reachability analysis. Many existing works encode human control behavior into a GMM using the Expectation-Maximization (EM) algorithm and have shown comparatively good performance. However, the conventional EM algorithm cannot address constraints on parameters other than the weight coefficients, so the trained GMM cannot explicitly account for given side information, e.g., the admissible control input ranges. To resolve this limitation, many variations of the EM algorithms have been proposed to address the constraints on the parameters, e.g., mean and covariance. For instance, the Gradient Projection (GP) EM algorithm employs the gradient projection algorithm to handle linear constraints [11]. The authors in [12] proposed the Expectation-Maximization-Projection (EMP) algorithm to handle linear and nonlinear equality constraints by adding the Projection step (P-step). In [13], the authors proposed a Sequential Quadratic Programming (SQP)-based EM algorithm that incorporates SQP in the conventional EM algorithm.

Motivated by the aforementioned works, this paper aims to probabilistically constrain the GMM within the admissible control input ranges. Moreover, we seek more accurate stochastic reachable sets that explicitly consider human control behavior and the admissible control input ranges. To this end, we confine the ellipsoidal confidence region of each Gaussian component by imposing a constraint related to the Mahalanobis distance using the SQP-based EM algorithm [13]. The Mahalanobis distance can be used to measure how far an observation is from a Gaussian distribution, where its absolute value corresponds to a confidence level following a χ-square distribution [14]. We design a constraint that restricts the Mahalanobis distance between the limits of admissible control input ranges and the Gaussian component

The authors would like to acknowledge that this work is supported by NSF CNS-1836952.

[1]Cheng-Han Yang, Joonwon Choi, Suriyan Anandavel, and Inseok Hwang are with School of Aeronautics and Astronautics, Purdue University, West Lafayette, IN 47907 USA {yang2323,choi774,sanandav,ihwang}@purdue.edu

(called *confidence region constraint*). The SQP-based EM algorithm is selected since the confidence region constraint is a nonlinear inequality which can be addressed efficiently by SQP [15]. Consequently, we can probabilistically constrain the GMM within the admissible control input ranges. We further analyze how the constrained GMM can improve the prediction of human control input and the stochastic reachable sets.

The contributions of this paper are as follows: 1) we propose constrained stochastic reachability analysis that can explicitly account for the admissible control input ranges of human control, 2) we present a mathematical analysis of how the confidence region constraint affects the predicted human control input by the GMR and the stochastic reachable sets, and 3) we perform a numerical simulation to compare the performance of stochastic reachable sets between the constrained and unconstrained human control behavior models.

This paper is organized as follows: In Section II, we provide the design preliminaries of the stochastic reachability analysis method, including control input prediction and the stochastic reachable sets computation. Section III presents the details of the EM algorithm and the confidence region constraints. A comprehensive mathematical analysis of the confidence level propagation from the human control behavior model to the reachability analysis is presented in Section IV. A numerical simulation is presented in Section V. Finally, we conclude our study in Section VI.

II. Reachability Analysis of a Human-in-the-Loop System

A. Human Control Behavior Modeling

This section presents the reachability analysis of the Human-in-the-Loop (HITL) system. In our previous work [1], we computed the close-loop stochastic reachable sets by modeling the human operator's control behavior as a Gaussian Mixture Model (GMM). In this paper, we consider the HITL system which can be represented as the following discrete-time linear time-invariant system:

$$\mathbf{x}_{k+1} = A\mathbf{x}_k + B\mathbf{u}_k, \tag{1}$$

where $\mathbf{x}_k \in \mathbb{R}^n$ and $\mathbf{u}_k \in \mathbb{R}^m$ are the state and control input vectors at time step k, and $A \in \mathbb{R}^{n\times n}$ and $B \in \mathbb{R}^{n\times m}$ are the state and input matrices, respectively. We assume the control input $\mathbf{u}_k$ is governed by a human operator in the HITL system (1). Thus, the human operator's control behavior needs to be modeled to compute the closed-loop stochastic reachable sets. To this end, we model such human control behavior as a GMM to address the uncertainty in human motion.

Considering a set of control input trajectories, which can be written as $\zeta := [\zeta_1^T, \zeta_2^T, ..., \zeta_K^T]$, where $\zeta_k = [t_k, \mathbf{u}_k^T]^T$, $t_k \in \mathbb{R}$ is the elapsed time at time step k ($k \in [1, ..., K]$), and K is the number of data, we encode human control behavior into a human control behavior model $\mathscr{M}$ as a GMM with ζ. The joint probability density function (PDF) of $\mathscr{M}$ can be written as:

$$P(\mathbf{u}, \mathbf{t}|\theta) = \sum_{j=1}^{L} w_j N(\mathbf{u}, \mathbf{t}|\mu_j, \Sigma_j), \tag{2}$$

where $\mathbf{u} = [\mathbf{u}_1^T, ..., \mathbf{u}_K^T]^T$, $\mathbf{t} = [t_1, ..., t_K]^T$, $w_j \in \mathbb{R}$ is the weight coefficients of the j-th component satisfying $\sum_{j=1}^{L} w_j = 1$, $\theta = [\theta_1, ..., \theta_L]^T$ is the parameter vector with $\theta_j := \{w_j, \mu_j, \Sigma_j\}$, $\mu_j \in \mathbb{R}^{m+1}$ and $\Sigma_j \in \mathbb{R}^{(m+1)\times(m+1)}$ are the mean and covariance matrix of the j-th component, respectively, and $N(\cdot|\mu_j, \Sigma_j)$ is the Gaussian PDF with parameters μ_j and Σ_j. L is the number of Gaussian components and can be heuristically determined based on various information criteria such as Bayesian Information Criterion (BIC) [16]. Throughout this paper, we assume that L is fixed. By applying the Expectation-Maximization (EM) algorithm, an optimal set of parameters θ can be estimated.

B. GMR for Reachability Analysis

Once $\mathscr{M}$ is trained as a GMM, the Gaussian Mixture Regression (GMR) can be used to predict how the human operator controls the system based on $\mathscr{M}$. In other words, the GMR provides the conditional PDF of the human control input at a given time step [7]. We only focus on the reachability analysis within $t_k \in [t_1, t_K]$, where t_1 and t_K denote the minimum and maximum elapsed time in ζ, respectively. The mean μ_j and covariance Σ_j of $\mathscr{M}$ are denoted as:

$$\mu_j = \begin{bmatrix} \mu_j^{\mathbf{u}} \\ \mu_j^{t} \end{bmatrix}, \Sigma_j = \begin{bmatrix} \Sigma_j^{\mathbf{u}} & \Sigma_j^{\mathbf{u}t} \\ \Sigma_j^{t\mathbf{u}} & \Sigma_j^{t} \end{bmatrix}, \tag{3}$$

where $\mu_j^{\mathbf{u}} \in \mathbb{R}^m$ and $\mu_j^t \in \mathbb{R}$ are the mean of the human control input and elapsed time, respectively, and $\Sigma_j^{\mathbf{u}}$, $\Sigma_j^{\mathbf{u}t}$, $\Sigma_j^{t\mathbf{u}}$, and Σ_j^t are the corresponding covariance fractions, respectively. The GMR prediction result, which provides the conditional PDF of the human control input at time step k, can be derived as [7]:

$$P(\mathbf{u}_k|t_k) = P(\mathbf{u}_k) = \sum_{j=1}^{L} \hat{w}_j(t_k) N(\mathbf{u}_k|\hat{\mu}_j(t_k), \hat{\Sigma}_j), \tag{4}$$

where

$$\hat{w}_j(t_k) = \frac{w_j N(t_k|\mu_j^t, \Sigma_j^t)}{\sum_{i=1}^{L} w_i N(t_k|\mu_i^t, \Sigma_i^t)}, \tag{5a}$$

$$\hat{\mu}_j(t_k) = \mu_j^{\mathbf{u}} + \Sigma_j^{\mathbf{u}t} {\Sigma_j^t}^{-1} (t_k - \mu_j^t) \tag{5b}$$

$$\hat{\Sigma}_j = \Sigma_j^{\mathbf{u}} - \Sigma_j^{\mathbf{u}t} {\Sigma_j^t}^{-1} \Sigma_j^{t\mathbf{u}}. \tag{5c}$$

With the conditional PDF (4) of human control input and the system dynamics (1), one-step propagation of the state PDF controlled by the human operator can be predicted by solving the Chapman–Kolmogorov equation as [1]:

$$P(\mathbf{x}_{k+1}) = \int_{\mathbf{x}_k} \sum_{j=1}^{L} \hat{w}_j(t_k) N(\mathbf{x}_{k+1}|A\mathbf{x}_k + B\hat{\mu}_j(t_k), B\hat{\Sigma}_j B^T) d\mathbf{x}_k. \tag{6}$$

By repeating this process up to the desired time step, t_f, one can compute the state PDF at t_f, $P(x_{t_f})$, which we define as the stochastic reachable sets of (1).

III. Side Information of Human Control Behavior

A. EM algorithm

A GMM is often trained by feeding ζ to the EM algorithm. The conventional EM algorithm is composed of Expectation-step (E-step) and Maximization-step (M-step) [17].

1) E-step: It computes the expectation of the complete-data log-likelihood with the posterior probability using the current parameters as follows:

$$l(\theta) := \sum_{j=1}^{L}\sum_{k=1}^{K} \gamma_{jk}^{s+1} \log(w_j N(\zeta_k|\mu_j,\Sigma_j)), \tag{7}$$

where γ_{jk}^{s+1} is the posterior probability that can be derived by the Bayes rule as:

$$\gamma_{jk}^{s+1} := \frac{w_j^s N(\zeta_k|\mu_j^s,\Sigma_j^s)}{\sum_{i=1}^{L} w_i^s N(\zeta_k|\mu_i^s,\Sigma_i^s)}, \tag{8}$$

where the superscript s denotes the sequence of iterations.

2) M-step: It maximizes the expectation (7) by updating the parameters as follows [17]:

$$w_j^{s+1} = \frac{\sum_{k=1}^{K}\gamma_{jk}^{s+1}}{K}, \tag{9a}$$

$$\mu_j^{s+1} = \frac{\sum_{k=1}^{K}\gamma_{jk}^{s+1}\zeta_k}{\sum_{k=1}^{K}\gamma_{jk}^{s+1}}, \tag{9b}$$

$$\Sigma_j^{s+1} = \frac{\sum_{k=1}^{K}\gamma_{jk}^{s+1}(\zeta_k-\mu_j^{s+1})(\zeta_k-\mu_j^{s+1})^T}{\sum_{k=1}^{K}\gamma_{jk}^{s+1}}. \tag{9c}$$

With the parameters updated in the M-step (9), one can update the posterior probability in (8). By repeating the E-step and the M-step until the convergence condition is met, an optimal set of parameters can be obtained. More details on the EM algorithm can be found [17], [18].

Although the conventional EM algorithm has shown good performance in many applications, it cannot handle parameter constraints other than weight coefficients. Therefore, to improve the performance of reachability analysis by explicitly accounting for given side information, such limitations need to be addressed.

B. Side Information and SQP-based EM Algorithm

In real-world applications, the magnitude of control input is typically constrained due to physical or mechanical limitations. Such admissible control input ranges can be considered as side information that can be described as follows:

$$-u_{max}^d \le u_k^d \le u_{max}^d, \quad \forall d \in [1,...,m], \tag{10}$$

where the superscript d denotes the d-th element of $\mathbf{u}_k$ and $u_{max}^d \in \mathbb{R}^+$ is its corresponding maximum magnitude. In this section, we aim to enforce the human control behavior model $\mathscr{M}$ to satisfy the following inequality:

$$P(-u_{max}^d \le u_k^d \le u_{max}^d) > \delta, \quad \forall d \in [1,...,m], \tag{11}$$

where $\delta \in [0,1]$ is the desired confidence level.

If the confidence region of each Gaussian component is confined within the admissible control input ranges (10), we can ensure that the entire GMM is also probabilistically constrained. Hence, we apply Sequential Quadratic Programming (SQP) to the EM algorithm to yield a GMM that can explicitly account for the control input constraints (11). The SQP-based EM algorithm has the same E-step in (7) but it maximizes the expectation using SQP as a modified M-step [13], which allows one to impose constraints on the parameters.

Furthermore, we can measure the Mahalanobis distance from each component to the bound of the admissible control input ranges. Such bounds are denoted as $\partial\mathbf{u}$, i.e., there exists at least one d such that $|\partial u^d| = u_{max}^d$, where ∂u^d is the d-th element of $\partial\mathbf{u}$. In other words, $\partial\mathbf{u}$ has at least one element equal to its corresponding maximum magnitude. If such Mahalanobis distance is constrained, we can ensure the confidence region of each component is confined within the admissible control input ranges. Therefore, we construct the confidence region constraint as follows:

$$\begin{aligned}&(\partial\mathbf{u}-\mu_j^{\mathbf{u}})^T\Sigma_j^{-1}(\partial\mathbf{u}-\mu_j^{\mathbf{u}}) \ge \alpha,\\ &\forall\partial\mathbf{u} \in \{\partial\mathbf{u}\in\mathbb{R}^m | \exists|\partial u^d| = u_{max}^d,\ d\in[1,...,m]\},\end{aligned} \tag{12}$$

where $\alpha := \chi^2(1-\delta,m)$ follows the χ-square distribution function with confidence level δ and m degree of freedom [19]. If the minimum value of $(\partial\mathbf{u}-\mu_j^{\mathbf{u}})^T\Sigma_j^{-1}(\partial\mathbf{u}-\mu_j^{\mathbf{u}})$ satisfies the above inequality, we can guarantee that the confidence region constraint (12) is automatically satisfied. Therefore, we search its minimum value in terms of d-th dimension, which yields:

$$(\pm u_{max}^d - \mu_j^d)^2/(\sigma_j^d)^2 \ge \alpha, \quad \forall d \in [1,...,m], \tag{13}$$

where $\mu_j^d \in \mathbb{R}$ is the d-th element of $\mu_j^{\mathbf{u}}$ and $(\sigma_k^d)^2 \in \mathbb{R}$ is the d-th diagonal value of $\Sigma_j^{\mathbf{u}}$.

By enforcing the constraints (13) with the SQP-based EM algorithm, one can guarantee that the human control behavior model $\mathscr{M}$ satisfies the control input constraints (11). Hence, the M-step of the SQP-based EM algorithm can be modified to solve the following constrained optimization problem:

$$\begin{aligned}\max_{\theta}\ & l(\theta) := \sum_{j=1}^{L}\sum_{k=1}^{K}\gamma_{jk}^{s+1}\log(w_j N(\zeta_k|\mu_j,\Sigma_j))\\ \text{subject to }& \sum_{j=1}^{L} w_j = 1,\\ & (\pm u_{max}^d - \mu_j^d)^2/(\sigma_j^d)^2 \ge \alpha, \quad \forall d\in[1,...,m].\end{aligned} \tag{14}$$

IV. Performance Analysis

A. GMR Prediction

In this section, we analyze the performance of the proposed scheme introduced in Section III. If a GMM is trained in a way that the constraints (13) are satisfied, we can measure the Mahalanobis distance from the mean of the j-th

component of the GMR prediction results (4) to $\partial \mathbf{u}$ in terms of the d-th dimension as:

$$\beta_j^d(t_k) := \min_{\partial \mathbf{u}} \ (\partial \mathbf{u} - \hat{\mu}_j(t_k))^T (\hat{\Sigma}_j)^{-1} (\partial \mathbf{u} - \hat{\mu}_j(t_k)),$$
$$\text{subject to } |\partial u^d| = u^d_{max}, \ \forall d \in [1, ..., m]. \tag{15}$$

In other words, the corresponding confidence level of $\beta_j^d(t_k)$ means the probability that the j-th component of the GMR prediction results (4) remains within the admissible control input ranges. In the rest of this subsection, we consider the case for $\partial u^d = u^d_{max}$ for notational simplicity and let $\overline{\beta_j^d}(t_k)$ denote the corresponding squared Mahalanobis distance since the same analysis can be applied to $\partial u^d = -u^d_{max}$. $\overline{\beta_j^d}(t_k)$ can be directly computed by the following equation:

$$\overline{\beta_j^d}(t_k) = (u^d_{max} - \hat{\mu}_j^d)^2 / (\hat{\sigma}_j^d)^2, \tag{16}$$

where $\hat{\mu}_j^d$ is the d-th element of $\hat{\mu}_j$ in (5b) and $(\hat{\sigma}_j^d)^2$ is the d-th diagonal value of $\hat{\Sigma}_j^{\mathbf{u}}$ in (5c). $\hat{\mu}_j^d$ and $(\hat{\sigma}_j^d)^2$ can be derived using (5) as:

$$\hat{\mu}_j^d(t_k) = \mu_j^d + (t_k - \mu_j^t)\sigma_j^{dt} / (\sigma_j^t)^2, \tag{17a}$$
$$(\hat{\sigma}_j^d)^2 = (\sigma_j^d)^2 - \left(\sigma_j^{dt} / \sigma_j^t\right)^2, \tag{17b}$$

where σ_j^{dt} is the d-th element of $\Sigma_j^{\mathbf{u}t}$ and σ_j^t is the square root of Σ_j^t. By substituting (17) into (16), we obtain:

$$\overline{\beta_j^d}(t_k) = \frac{1}{1-(\rho_j^d)^2} \left(\frac{u^d_{max} - \mu_j^d}{\sigma_j^d} - \rho_j^d \frac{t_k - \mu_j^t}{\sigma_j^t} \right)^2, \tag{18}$$

where $\rho_j^d := \sigma_j^{dt} / \sigma_j^d \sigma_j^t$ is the correlation coefficient of u_k^d and t_k of the j-th component.

To see how the proposed method improves the GMR prediction results, we are interested in the value of $\overline{\beta_j^d}(t_k)$. Since we do not impose constraints regarding the correlation between $\mathbf{u}_k$ and t_k, but $\overline{\beta_j^d}(t_k)$ can be affected by it, we search its infimum with respect to ρ_j^d to understand how likely the conditional PDF of the GMR prediction results remain within the admissible control input ranges after imposing the confidence region constraints.

For a given t_k and the fact that $\rho_j^d \in [-1, 1]$, the infimum of $\overline{\beta_j^d}(t_k)$ can be derived by taking the derivative with respect to ρ_j^d equal to zero as:

$$\inf_{\rho_j^d} \overline{\beta_j^d}(t_k) = \ \max \left(0, \frac{(u^d_{max} - \mu_j^d)^2}{(\sigma_j^d)^2} - \frac{(t_k - \mu_j^t)^2}{(\sigma_j^t)^2} \right). \tag{19}$$

The infimum of $\overline{\beta_j^d}(t_k)$ is then discussed under two cases. First, if the following inequality holds:

$$\frac{(u^d_{max} - \mu_j^d)^2}{(\sigma_j^d)^2} \ \geq \ \frac{(t_k - \mu_j^t)^2}{(\sigma_j^t)^2}, \tag{20}$$

its corresponding infimum of $\overline{\beta_j^d}(t_k)$ can be obtained by enforcing the constraints (13) as:

$$\inf_{\rho_j^d} \overline{\beta_j^d}(t_k) = \alpha - \frac{(t_k - \mu_j^t)^2}{(\sigma_j^t)^2}. \tag{21}$$

Second, for the case that

$$\frac{(t_k - \mu_j^t)^2}{(\sigma_j^t)^2} \ > \ \frac{(u^d_{max} - \mu_j^d)^2}{(\sigma_j^d)^2}, \tag{22}$$

its corresponding infimum of $\overline{\beta_j^d}(t_k)$ is 0. One can easily notice that if the magnitude of $(t_k - \mu_j^t)/\sigma_j^t$ increases from (21), the infimum of $\overline{\beta_j^d}(t_k)$ will significantly decrease or even become 0 if it satisfies (22). Nevertheless, it is worth noting that the magnitude of $(t_k - \mu_j^t)/\sigma_j^t$ increases only when the current time step t_k deviates significantly from μ_j^t. In this case, we can observe from (5a) that the conditional weight $\hat{w}_j(t_k)$ of the corresponding Gaussian component also significantly decreases. This means that the GMR prediction result (4) is mostly contributed by other dominant components. Accordingly, although we cannot guarantee the confidence region of the j-th component remains within the admissible control input ranges, its influence on the overall conditional PDF is relatively small. In addition, since the constraints (13) are also satisfied for $\partial u^d = -u^d_{max}$, the analysis from (16) to (22) also holds for this case. This will also be demonstrated through a numerical simulation in the following section.

B. Stochastic Reachable Sets

In this subsection, we analyze the Mahalanobis distance of the stochastic reachable sets based on the human control behavior model $\mathscr{M}$ that satisfies the constraints (13). Given the HITL system dynamics (1), the admissible control input ranges (10), and the current state $\mathbf{x}_k$, one can derive the boundary of the reachable sets at time step $k+1$ as:

$$\mathscr{R}_{k+1} := A\mathbf{x}_k + B\partial \mathbf{u},$$
$$\forall \partial \mathbf{u} \in \{\partial \mathbf{u} \in \mathbb{R}^m | \exists |\partial u^d| = u^d_{max}, \ d \in [1, ..., m]\}, \tag{23}$$

With the human control behavior model $\mathscr{M}$ that satisfies (13), one can derive the one-step stochastic reachable sets using (6) as [1]:

$$P(\mathbf{x}_{k+1}) = \sum_{j=1}^{L} \hat{w}_j(t_k) N(\mathbf{x}_{k+1} | A\mathbf{x}_k + B\hat{\mu}_j(t_k), B\hat{\Sigma}_j B^T) \tag{24}$$

Same as (15), we measure the Mahalanobis distance from the j-th component of the stochastic reachable sets to $\mathscr{R}_{k+1}$ in terms of the d-th dimension of $\mathbf{u}_k$ as:

$$\psi_j^d(t_k) := \min_{\partial \mathbf{u}} \ (\mathscr{R}_{k+1} - \tilde{\mu}_j(t_k))^T (\tilde{\Sigma}_j)^{-1} (\mathscr{R}_{k+1} - \tilde{\mu}_j(t_k)),$$
$$\text{subject to } |\partial u^d| = u^d_{max}, \ \forall d \in [1, ..., m], \tag{25}$$

where

$$\tilde{\mu}_j(t_k) = A\mathbf{x}_k + B\hat{\mu}_j(t_k),$$
$$\tilde{\Sigma}_j = B\hat{\Sigma}_j B^T. \tag{26}$$

By substituting (26) into (25), one can see that $\psi_j^d(t_k)$ is exactly equal to $\beta_j^d(t_k)$. Therefore, both the GMR prediction results and the stochastic reachable sets based on the human control behavior model $\mathscr{M}$ are probabilistically constrained in terms of the admissible control input ranges with a confidence level that corresponds to $\beta_j^d(t_k)$.

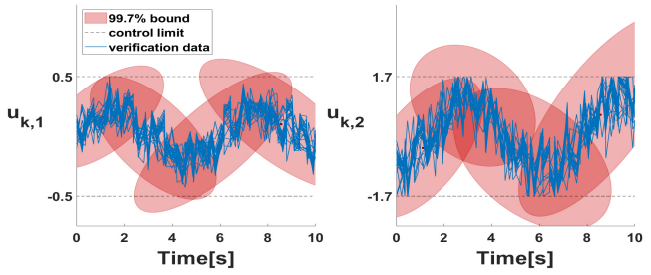

(a) Unconstrained GMM [17]

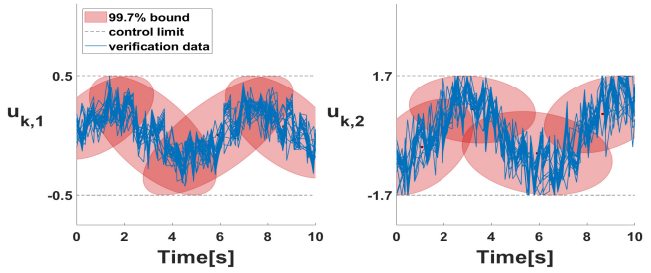

(b) Constrained GMM

Fig. 1: Comparison of the Gaussian components between the unconstrained and constrained GMMs

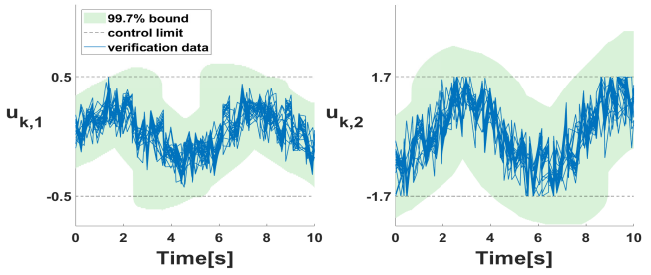

(a) GMR predictions of unconstrained GMM

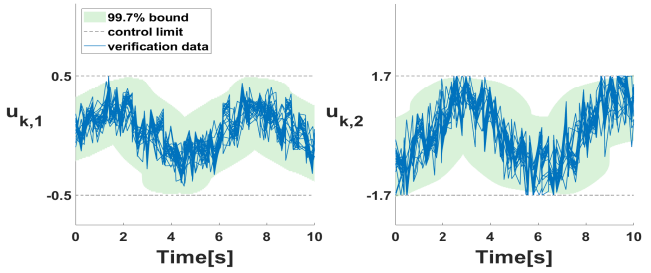

(b) GMR predictions of constrained GMM

Fig. 2: GMR prediction results comparison between the unconstrained and constrained models

V. Numerical Simulation

A. Simulation Environment

To demonstrate the effectiveness of the proposed algorithm, we randomly generate 80 training sets and 30 validation sets using the following equation:

$$\mathbf{u}_k(t_k) = \begin{bmatrix} 0.2(\sin(t_k) + N(0,0.5)) \\ -(\cos(t_k) + N(0,0.5)) \end{bmatrix}, \tag{27}$$

where t_k is uniformly distributed within $t_k \in [0,10]s$ and $N(0,0.5)$ is the Gaussian noise term with mean 0 and standard deviation 0.5. In addition, we intentionally substitute t_k with $t_k + 0.2$ for $1/5$ of the dataset to increase the uncertainties. The state and input matrices of the HITL system (1) are given as:

$$A = \begin{bmatrix} 0.99 & 0 \\ 0 & -0.2 \end{bmatrix}, \quad B = \begin{bmatrix} -0.36 & 0.16 \\ 4 & -0.24 \end{bmatrix}, \tag{28}$$

with the current state $\mathbf{x}_k = [x_{k,1}, x_{k,2}]^T$ and the control input $\mathbf{u}_k = [u_{k,1}, u_{k,2}]^T$. The number of Gaussian components is fixed as $L = 4$, and the desired confidence level is set to be $\delta = 99.7\%$, which can be changed as necessary. The admissible control input ranges are $u_{k,1} \in [-0.5, 0.5]$ and $u_{k,2} \in [-1.7, 1.7]$, respectively, and we focus on the reachability analysis within $t_k \in [0,10]s$.

B. GMM Training

We encode the training dataset into two GMMs separately. One is trained using the conventional EM algorithm [17], and the other is trained with the confidence region constraints (13) imposed.

Figure 1 shows the 99.7% confidence regions of each component of the unconstrained and constrained GMMs, respectively. The red ellipses represent the 99.7% confidence region of each component, the blue lines represent the verification dataset, and the dashed lines represent the limits of $u_{k,1}$ and $u_{k,2}$. Figure 1b shows that the 99.7% confidence regions of each component in the constrained GMM are bounded within the admissible ranges of $u_{k,1}$ and $u_{k,2}$, while those of the unconstrained GMM exceed the bounds at most time steps, which can be observed in Figure 1a.

C. Prediction of Control Input Using GMR

This subsection presents the human operator control input prediction using the GMR with the GMMs from the previous subsection. In Figure 2, the green area represents the 99.7% confidence bounds of the GMR prediction results (4), where the probability of the state located within the bound is 99.7%. The blue lines and black dashed lines are the same as in Fig. 1.

Fig. 2 shows that the prediction based on the unconstrained GMM has a much higher chance of exceeding the admissible ranges of $u_{k,1}$ and $u_{k,2}$ than the constrained GMM since the significant portion of the 99.7% bounds (green area) of the unconstrained GMM are over the admissible control input bounds while that of the constrained GMM are all within the admissible bounds. This can be easily observed at $t_k \in [2,8]s$ for $u_{k,1}$ and the entire time horizon for $u_{k,2}$, respectively. On the other hand, Figure 2b shows a more concentrated prediction that the 99.7% confidence bound of the prediction is within the admissible control input ranges for the entire time horizon.

D. Stochastic Reachable Sets

Given the current state $\mathbf{x}_k = [0,0]^T$, the HITL system dynamics (1), and the GMR prediction results from the previous subsection, we can compute the PDF of the following

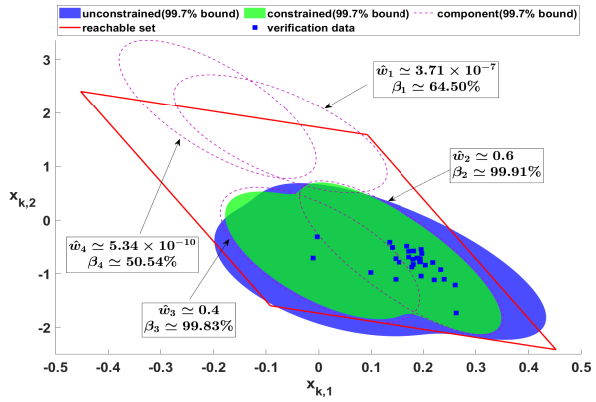

Fig. 3: Reachable sets comparison between the unconstrained and constrained models at $t_k = 4.3[s]$

state $\mathbf{x}_{k+1}$ as $P(\mathbf{x}_{k+1})$ using (6). As an example, Figure 3 compares the stochastic reachable sets at $t_k = 4.3[s]$. The red quadrilateral is the boundary of the reachable sets based on the HITL system dynamics and the admissible ranges of $u_{k,1}$ and $u_{k,2}$. The blue and green areas are the 99.7% confidence bounds of the stochastic reachable sets using the unconstrained and constrained GMMs, respectively. The blue squares are the verification data, and the pink dashed lines are the 99.7% confidence regions of each component of $P(\mathbf{x}_{k+1})$ based on the constrained GMM. As one can easily notice, the proposed method results in the stochastic reachable sets whose 99.7% confidence bound is well-included within the boundary of reachable sets, whereas those based on unconstrained GMM exceed the boundary.

Meanwhile, $\hat{w}$ is the weight coefficient (5a), and β is the corresponding confidence level of the minimum squared Mahalanobis distance from each component to the red quadrilateral (25), where the subscript $j = [1, ..., 4]$ denotes the sequence of components. Although the 99.7% confidence regions of two components exceed the boundary, their weight is relatively low ($\hat{w}_1 \simeq 10^{-7}$ and $\hat{w}_4 \simeq 10^{-10}$). Thus, the resultant $P(\mathbf{x}_{k+1})$ is dominated by the other two components, which remain within the boundary. This result aligns with the analysis in the previous section that those components with higher $\hat{w}$ are guaranteed to have a higher infimum of β. Accordingly, the proposed algorithm is shown to yield a more accurate prediction that can be applied to improve the efficiency and reliability of HITL systems.

VI. Conclusion

This paper proposed a constrained reachable analysis for Human-in-the-Loop (HITL) that can explicitly account for the admissible control input ranges of the human operator. We modeled the human control behavior as a constrained Gaussian Mixture Model (GMM) by confining the confidence regions of each component using Sequential Quadratic Programming (SQP). Then, the control input of the human operator was predicted using Gaussian Mixture Regression (GMR) and the stochastic reachable sets were computed using the Chapman–Kolmogorov equation. Through the numerical simulation, we demonstrated that the GMM can be probabilistically constrained within the admissible control input ranges by a desired confidence level using the SQP-based Expectation-Maximization (EM) algorithm. Furthermore, we derived the corresponding confidence level of the GMR prediction results and the stochastic reachable sets, which were also shown to be probabilistically constrained within their corresponding admissible ranges.

References

[1] Choi, J., Byeon, S., & Hwang, I. (2022). State prediction of human-in-the-loop multi-rotor system with stochastic human behavior model. IFAC-PapersOnLine, 55(41), 119-124.

[2] Lu, Z., Hong, H., Gerdts, M., & Holzapfel, F. (2022). Flight Envelope Prediction via Optimal Control-Based Reachability Analysis. Journal of Guidance, Control, and Dynamics, 45(1), 185-195.

[3] Koert, D., Pajarinen, J., Schotschneider, A., Trick, S., Rothkopf, C., & Peters, J. (2019). Learning intention aware online adaptation of movement primitives. IEEE Robotics and Automation Letters, 4(4), 3719-3726.

[4] Wang, W., Xi, J., & Zhao, D. (2018). Learning and inferring a driver's braking action in car-following scenarios. IEEE Transactions on Vehicular Technology, 67(5), 3887-3899.

[5] Luo, R., & Berenson, D. (2015, September). A framework for unsupervised online human reaching motion recognition and early prediction. In 2015 IEEE/RSJ International Conference on Intelligent Robots and Systems (IROS) (pp. 2426-2433). IEEE.

[6] Hou, B., He, Z., Wang, J., Sun, B., & Zhang, K. (2017, May). A new fault diagnosis method based on component-wise expectation-maximization algorithm and K-means algorithm. In 2017 6th Data Driven Control and Learning Systems (DDCLS) (pp. 776-781). IEEE.

[7] Calinon, S. (2016). A tutorial on task-parameterized movement learning and retrieval. Intelligent service robotics, 9, 1-29.

[8] Khansari-Zadeh, S. M., & Billard, A. (2011). Learning stable nonlinear dynamical systems with gaussian mixture models. IEEE Transactions on Robotics, 27(5), 943-957.

[9] Mainprice, J., & Berenson, D. (2013, November). Human-robot collaborative manipulation planning using early prediction of human motion. In 2013 IEEE/RSJ International Conference on Intelligent Robots and Systems (pp. 299-306). IEEE.

[10] Govindarajan, V., Driggs-Campbell, K., & Bajcsy, R. (2017, December). Data-driven reachability analysis for human-in-the-loop systems. In 2017 IEEE 56th Annual Conference on Decision and Control (CDC) (pp. 2617-2622). IEEE.

[11] Jamshidian, M. (2004). On algorithms for restricted maximum likelihood estimation. Computational statistics & data analysis, 45(2), 137-157.

[12] Takai, K. (2012). Constrained EM algorithm with projection method. Computational statistics, 27, 701-714.

[13] Li, B., Liu, W., & Dou, L. (2010). Unsupervised learning of Gaussian mixture model with application to image segmentation. Chinese Journal of Electronics, 19(3), 451-456.

[14] Gallego, G., Cuevas, C., Mohedano, R., & Garcia, N. (2013). On the Mahalanobis distance classification criterion for multidimensional normal distributions. IEEE Transactions on Signal Processing, 61(17), 4387-4396.

[15] Powell, M. J. (2006, August). A fast algorithm for nonlinearly constrained optimization calculations. In Numerical Analysis: Proceedings of the Biennial Conference Held at Dundee, June 28–July 1, 1977 (pp. 144-157). Berlin, Heidelberg: Springer Berlin Heidelberg.

[16] McLachlan, G. J., & Rathnayake, S. (2014). On the number of components in a Gaussian mixture model. Wiley Interdisciplinary Reviews: Data Mining and Knowledge Discovery, 4(5), 341-355.

[17] Zhang, Y., Li, M., Wang, S., Dai, S., Luo, L., Zhu, E., ... & Zhou, H. (2021). Gaussian mixture model clustering with incomplete data. ACM Transactions on Multimedia Computing, Communications, and Applications (TOMM), 17(1s), 1-14.

[18] Dempster, A. P., Laird, N. M., & Rubin, D. B. (1977). Maximum likelihood from incomplete data via the EM algorithm. Journal of the royal statistical society: series B (methodological), 39(1), 1-22.

[19] Wang, B., Shi, W., & Miao, Z. (2015). Confidence analysis of standard deviational ellipse and its extension into higher dimensional Euclidean space. PloS one, 10(3), e0118537.